Revealing the nonlinear response of a tunneling two-level system ensemble using coupled modes

Naftali Kirsh, Elisha Svetitsky, Alexander L. Burin, Moshe Schechter, and Nadav Katz

Revealing the nonlinear response of a tunneling two-level system ensemble using coupled modes

Naftali Kirsh,[1] Elisha Svetitsky,[1] Alexander L. Burin,[2] Moshe Schechter,[3] and Nadav Katz[1]

[1]*Racah Institute of Physics, the Hebrew University of Jerusalem, Jerusalem, 91904 Israel*
[2]*Department of Chemistry, Tulane University, New Orleans, Louisiana 70118, USA*
[3]*Department of Physics, Ben-Gurion University of the Negev, Beer Sheva 84105, Israel*
(Dated: May 7, 2017)

Atomic sized two-level systems (TLSs) in amorphous dielectrics are known as a major source of loss in superconducting devices. In addition, individual TLS are known to induce large frequency shifts due to strong coupling to the devices. However, in the presence of a broad ensemble of TLSs these shifts are symmetrically canceled out and not observed in a typical single-tone spectroscopy experiment. We introduce a two-tone spectroscopy on the normal modes of a pair of coupled superconducting coplanar waveguide resonators to reveal this effect. Together with an appropriate saturation model this enables us to extract the average single-photon Rabi frequency of dominant TLSs to be $\Omega_0/2\pi \approx 79$ kHz. At high photon numbers we observe an enhanced frequency shift due to nonlinear kinetic inductance when using the two-tone method and estimate the value of the nonlinear coefficient as $K/2\pi \approx -1 \times 10^{-4}$ Hz/photon. Furthermore, the life-time of each resonance can be controlled (increased) by pumping of the other mode as demonstrated both experimentally and theoretically.

The characterization of a nonlinear medium often involves the usage of a strong (pump) field which modifies the medium properties, combined with a weak (probe) field which is used for measurement. When the nonlinear response of a resonant device is probed, the finite linewidth limits the available pumping bandwidth and thus might hide the full nonlinear behavior. Here we show how this problem can be solved by using the normal modes of a coupled system. When two modes share the same spatial volume but have different frequencies, one mode can be pumped strongly, modifying the medium locally overlapping with the other mode which is used for probing. When the splitting between the modes is large enough the pumped mode can modify the spectral components of the medium outside of the other mode's linewidth. In this Rapid Communication we demonstrate how this method can reveal nonlinear properties which would have remained hidden even for the strongest drive possible if the standard method was used. In particular, we measure low-power nonlinear frequency shifts of resonances formed by coupled superconducting coplanar waveguide resonators (CPWR)[1]. As we show, these shifts, caused by pumping at a detuning of ~ 1000 times the resonance linewidth, are well explained by the saturation of two-level systems (TLSs) in the device's dielectrics. Thus, this method can be used to give valuable information about TLSs, which was unavailable otherwise. Furthermore, at high powers, when kinetic inductance nonlinearity is dominant, our two-tone method provides twice the nonlinear sensitivity, which might be useful for applications such as microwave kinetic inductance detectors[2] and resonators' frequency tuning[3].

Investigated in the context of amorphous material physics[4–6], TLSs in dielectrics were brought into focus again since the discovery of their critical role as a loss mechanism in superconducting devices[7]. While the effect of TLSs saturation by probe power on the imaginary part of the dielectric constant $Im\,(\epsilon)$ (i.e. internal loss) was investigated thoroughly[7–13], the modification of $Re\,(\epsilon)$ (i.e. frequency shift) by the drive has remained hidden[14]. Here we demonstrate how by applying a pump-probe measurement on coupled modes this effect can be revealed.

Coupled resonators with a strong Josephson nonlinearity were used e.g. for quantum-limited amplification[17], stabilization of photon-number states[18] and for simulating a Bose-Hubbard chain[19]. Here we use coupled resonators as a tool to characterize the intrinsic nonlinearities of the resonators. For an ideal coupled pair of two identical resonators the normal modes will be a symmetric mode and an antisymmetric one for which the wave functions are identical up to a phase. This allows us to ignore uncertainties e.g. in electric field distribution and treat the modes referring only to the ability to saturate detuned spectral components of the nonlinear medium (see Fig. 1).

Our device consists of two capacitively coupled $\lambda/2$ CPWR made from ~ 120 nm Al sputtered on high-resistivity Silicon ($\rho > 5000$ $\Omega\cdot$cm), see Fig. 1. These resonators are physically identical, hence their bare (uncoupled) resonance frequencies are the same, but due to the coupling, two modes split by ~ 63 MHz at 5626 and 5689 MHz are formed. We characterize the resonances by measuring the transmission through a common feedline to which they are capacitively coupled using a vector network analyzer. The resonance frequency f_0, internal quality factor Q_i and the steady-state average number of photons $\langle N \rangle$ stored in the resonator are extracted by fitting the complex transmission data $S_{21}(f)$ to an appropriate model[20–23]. In order to quantify the nonlinear response of the resonances the probe power is scanned at a range which corresponds to $\langle N \rangle = 10^1 - 10^8$ photons, and the dependence of various parameters on $\langle N \rangle$ is analyzed. All measurements were conducted at a tem-
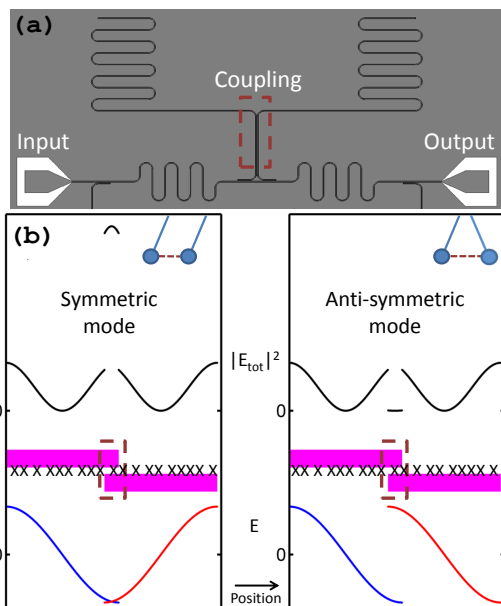
FIG. 1. (a) Design of the coupled resonators device[15]. Empty area represents Si substrate, gray area represents metal (Al). Feedline and resonators are black for clarity. Dark-red dashed box marks the coupling region. (b) Cartoon of the experimental idea. Magenta bars represent the resonators, the x axis is the position along their lengths. In analogy to coupled pendula the coupling results in the forming of a symmetric and an antisymmetric modes which differ only by the phase between the electric fields in both resonators (blue and red curves)[16]. TLSs (represented by 'X') experience the same total field intensity (black curves) in both modes, except for the small coupling area in which the resonators' fields interfere. This allows ignoring other details than the frequency detuning between the modes.

perature of ~ 20 mK with the device mounted to the base plate of a dilution refrigerator.

In Fig. 2 we show the resonance frequency f_0 and internal loss $1/Q_i$ of the resonances obtained using the standard single-tone spectroscopy method (for a uniform medium and electric field $1/Q_i = \tan\delta$, the bulk loss tangent, see[23]). The frequency of a single-tone probe is scanned around one resonance for various probe powers and the parameters are extracted as detailed above. As shown in Fig. 2b the loss dependence on $\langle N \rangle$ agrees well with the TLS model[23]. In addition, as predicted by this model[9], for stored energies corresponding to $\langle N \rangle \lesssim 10^5$ there is no observable frequency shift. For higher probe powers there is a strong negative shift which depends linearly on the number of photons. This linear shift is explained as resulting from nonlinear kinetic inductance[24] which can be modeled as a Kerr nonlinearity[25] (the weak negative shift for $10^5 \lesssim \langle N \rangle \lesssim 10^7$ resulting in a discrepancy from the fits at low powers might be due to the finite number of TLSs, see[23]). We elaborate more on the high power regime below. We stress here that in fact TLSs far detuned from resonance contribute to the real part of the dielectric constant ϵ[9] and therefore should effect

f_0, but because the standard method uses a single tone which saturates TLSs symmetrically around resonance this nonlinear effect is effectively hidden (See Figs. 4a and 4b).
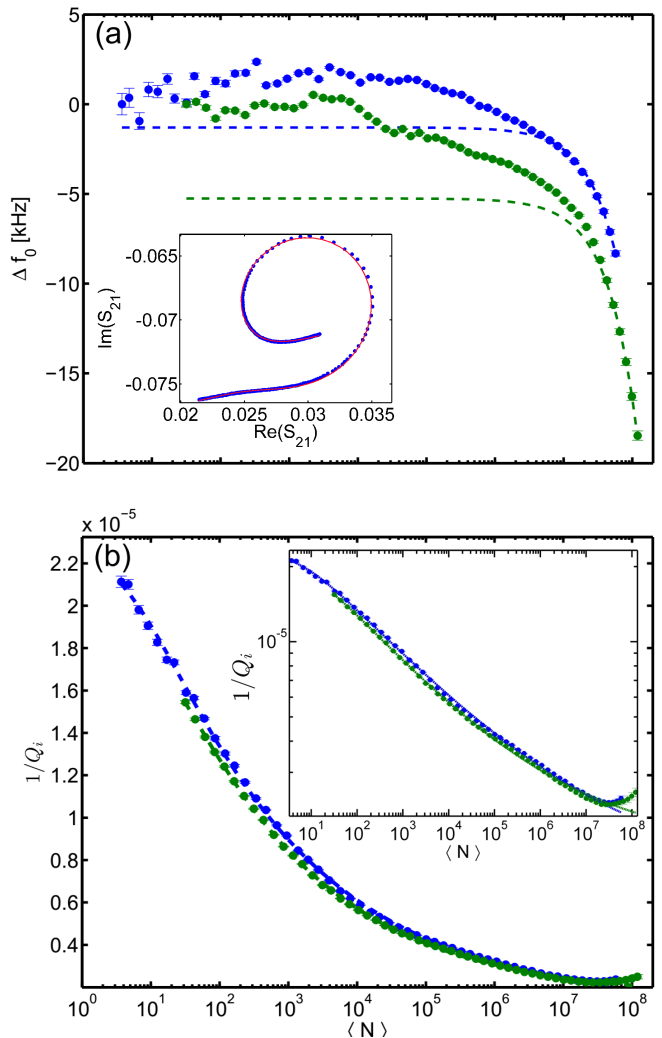

FIG. 2. (a) Resonance frequency shift and (b) Internal loss (shown in a log-log scale in the inset) vs $\langle N \rangle$ for the probe-only experiment for the resonances at 5626 MHz (green) and 5689 MHz (blue). Dashed lines in 2a are linear fits of the high power shifts to a Kerr nonlinearity model as detailed in the text. Dashed lines in 2b are fits to the standard TLS model ([23] Eq. (29)). Inset in Fig. 2a: a typical fit of the transmission data.

The full nonlinear behavior of the resonances is revealed when we use our two-tone pump-probe method. This is done by pumping strongly at a frequency close to one resonance while measuring $S_{21}(f)$ of the other resonance using a weak probe. Fig. 3a shows the results of this experiment. Notice that while in Fig. 2 the x axis indicates the average number of photons in the *probed* resonance, in Fig. 3 the x axis shows the average number of photons in the *pumped* resonance and the weak probe power is held constant[23]. In contrary to the kinetic in-

ductance nonlinearity at high photon numbers which is common to both types of experiments, at lower powers there is a significant frequency shift in the pump-probe experiments which is not observed in the probe-only experiments. Furthermore, the direction of the resonance shift depends on the relative position of the pumped and probed resonances. A negatively-detuned pump induces a negative shift on the probed resonance and vice-versa. These shifts can be explained by generalizing the TLS model to the pump and probe case. We first give a qualitative explanation of the physical reasoning behind the differences and then give the details of the full derivation. The effect of one TLS on the probed mode fre-

FIG. 4. Qualitative picture of the generalized TLS saturation model for the resonance shift. A black 'X' represents a TLS. A red 'X' represents a saturated TLS. Green arrows represent the level repulsion (the length indicating the repulsion strength). Red arrows represent the pump tone. (a) In the absence of pumping the TLSs are symmetrically distributed around a resonance, resulting in a broadening without a frequency shift. (b) A symmetric pump around one resonance narrows the linewidth without a frequency shift. (c) When two resonances are present, strongly pumping symmetrically around the lower resonance results in an asymmetric repulsion for the higher resonance, causing a frequency shift. (d) When the pump power increases, the repulsion of the higher resonance becomes more and more symmetric, causing a decrease in the frequency shift.
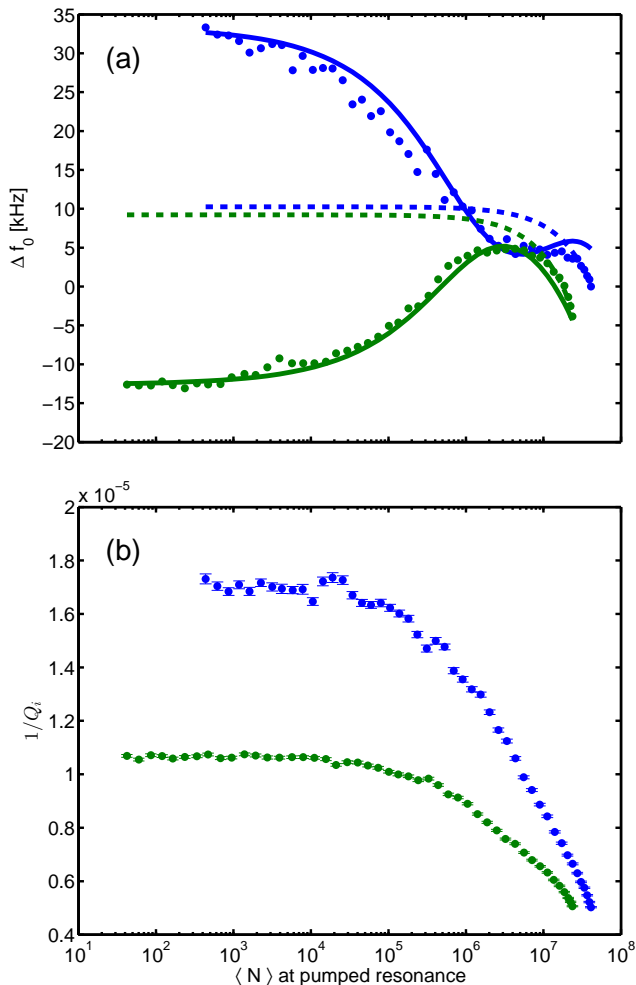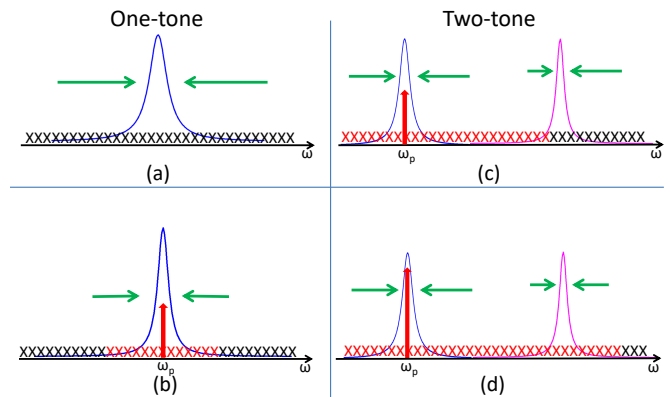

FIG. 3. (a) Resonance frequency shift and (b) Internal loss vs the average number of photons $\langle N \rangle$ in the pumped mode for the pump-probe experiment. Green (blue) points are for probe at 5626 MHz (5689 MHz) and pump at 5689 MHz (5626 MHz). The dashed lines in Fig. 3a are linear fits of the high power shifts to a Kerr nonlinearity model as detailed in the text. Solid lines are sums of the fits to the prediction of the generalized model of frequency shift due to TLSs (Eq. (4)) and the linear fits. In Fig. 3a constant shifts were added for clarity.

quency can be approximately described by the dispersive shift[26] $\Delta\omega_{pr} = \frac{g^2}{\Delta}\langle\hat{S}_z\rangle$, where g is the coupling strength between the TLS and the mode, $\Delta \equiv \omega_{TLS} - \omega_{pr}$ is their detuning and $\hat{S}_z = \pm 1$ is a TLS state operator (this result is obtained by applying second order perturbation theory on the Jaynes-Cummings Hamiltonian[27], assuming $g < \Delta$ and can be understood as resulting from level repulsion between the mode and the TLS). Since TLSs density of states is uniform in energy[6] they will be distributed symmetrically around ω_{pr} resulting in equal negative and positive shifts which sum to a zero shift with a broadened linewidth (Fig. 4a). When a TLS is pumped strongly it populates the excited state half of the time, yielding $\langle\hat{S}_z\rangle = 0$. Nevertheless, when the standard probe-only method is used, TLSs are saturated symmetrically around ω_{pr}, hence the effect is only linewidth narrowing (i.e. reducing the internal loss) but no observable frequency shift (Fig. 4b). The situation is different when one mode is pumped while the other is probed. The presence of another mode opens a spectral window for asymmetric saturation of TLSs which effects the probed mode due to the spatial coexistence of both modes' fields. When a mode negatively (positivity) detuned from the probe field is pumped strongly TLSs negatively (positivity) detuned from ω_{pr} are saturated, while positivity (negatively) detuned TLSs are less affected, resulting in a negative (positive) net shift (Fig. 4c). Increasing pump power increases also the TLSs satura-

tion (from power broadening), initially increasing the shift but eventually making saturation more and more symmetric, hence reducing the shift (Fig. 4d). We now present a full quantitative model to explain the results[23]. A single TLS is characterized by an asymmetry energy Δ_j, a tunneling amplitude Δ_{0j} resulting in the eigenenergy $E_j \equiv \hbar\omega_j \equiv \sqrt{\Delta_j^2 + \Delta_{0j}^2}$ and an electric dipole moment p_j[6]. The dipole coupling coefficient to a uniform electric field occupying a volume V filled by a material with a dielectric constant ϵ is $g_j \equiv \frac{\cos\theta_j p_j \sqrt{\omega_{pr}}}{\sqrt{2\hbar\epsilon\epsilon_0 V}} \frac{\Delta_{0j}}{\hbar\omega_j}$, where θ_j is the angle between the electric field and the dipole and ω_{pr} is the probed mode frequency. Summing contributions from all TLSs we obtain the frequency shift

$$\Delta\omega_{pr} = \mathrm{Re}\left[\sum_j g_j^2 \frac{\langle\hat{S}_{z,j}\rangle}{\omega_j - \omega_{pr} + \frac{i}{T_{2j}}}\right], \qquad (1)$$

where $T_{2j} = 2T_{1j}$ are the relaxation and dephasing times of the TLS (assuming a negligible TLS-TLS interaction). The population difference induced by pumping yields[6]

$$\langle\hat{S}_{z,j}\rangle = -\tanh\left(\frac{\hbar\omega}{2k_B T}\right) \times$$

$$\left(1 - \frac{T_{1j}\Omega_{Rj}^2/T_{2j}}{(\omega_j - \omega_{pump})^2 + T_{2j}^{-2}\left(1 + \Omega_{Rj}^2 T_{1j} T_{2j}\right)}\right) \quad (2)$$

where ω_{pump} is the pump frequency and the TLS Rabi frequency due to pumping is given by

$$\Omega_{Rj} \equiv \frac{\Delta_{0j}}{\hbar\omega_j}\cos\theta_j \Omega_0, \quad \hbar\Omega_0 \equiv 2p_j F_{pump}, \qquad (3)$$

with the pump field F_{pump}. Using the standard TLS model distribution we obtain that in the strong field regime $\Omega_0 T_1 T_2 \gg 1$ the frequency shift due to pumping is[23]

$$\frac{\Delta\omega_{pr}}{\omega_{pr}\tanh\left(\frac{\hbar\omega_{pr}}{2k_B T}\right)} = \frac{\sqrt{2}P_0 p^2 \pi^2}{8\epsilon\epsilon_0}\frac{\Delta\omega}{\Omega_0}\frac{\sqrt{1 + \frac{\Omega_0^2}{2\Delta\omega^2}} - 1}{\sqrt{1 + \frac{\Omega_0^2}{2\Delta\omega^2}} + 1}, \tag{4}$$

where $\Delta\omega \equiv \omega_{pump} - \omega_{pr}$ is the detuning between the pump and probe frequencies and P_0 is the TLSs density of states. As expected from the qualitative picture, for small fields ($\Omega_0 \ll \Delta\omega$) the shift increases with $\langle N \rangle$ as $\Delta\omega_{pr} \propto \Omega_0 \propto \sqrt{\langle N \rangle}$, while it decreases as $\Delta\omega_{pr} \propto \Omega_0^{-1} \propto \langle N \rangle^{-\frac{1}{2}}$ for high fields ($\Omega_0 \gg \Delta\omega$). In addition, the direction of the shift follows the sign of $\Delta\omega$[23] as expected. In Fig. 3a we show fits to this model for both resonances[23]. From the fits we obtain an estimate to the average single photon Rabi frequency of a dominant TLS $\Omega_0^{N=1}/2\pi \approx 79$ kHz[23]. These values confirm the predictions of previous studies[28,29] and of our Monte-Carlo simulations[23] that TLSs at regions of strong fields dominate the nonlinear behavior. In comparison to the frequency shift the internal loss needs a much

larger number of photons to show a significant response (Fig. 3b), This agrees with our theoretical calculations[23] and demonstrates the fact that the imaginary part of ϵ is only sensitive to nearly resonant TLSs[9].

As mentioned above, for large $\langle N \rangle$ a negative frequency shift is observed in both probe-only and pump-probe experiments. This shift can be attributed to nonlinear kinetic inductance[24] which might be explained e.g. as resulting from quasiparticle microwave heating[30] or modification of the superconducting ground state by the field[31]. Following Yurke and Buks[25] we model this effect as a Kerr nonlinearity, resulting in a frequency shift which is linear in the number of photons

$$\Delta f_0 = \frac{K}{2\pi}\langle N \rangle, \tag{5}$$

where K is the Kerr coefficient. A linear fit to the single-tone experiments high-power frequency shifts (Fig. 2a) yields $\frac{K}{2\pi} = -1.11(0.05) \times 10^{-4}$ Hz/photon for the resonance at 5626 MHz and $\frac{K}{2\pi} = -1.23 \times 10^{-4}$ Hz/photon for the resonance at 5689 MHz. These results agree with order of magnitude estimations based on a simple nonlinear kinetic inductance model[23]. These close values for both resonances agree with the fact that kinetic inductance should depend on the superconducting Al properties[30–32]. Generalizing the model to the case of coupled resonators[23] we find that the expected shift of one resonance due to photons in the other resonance is linear in the number of photons with the coefficient $K' = 2K$, i.e. doubled. Fitting the two-tone experiments high-power frequency shifts (Fig. 3a) we obtain $\frac{K'}{2\pi} = -5(1) \times 10^{-4}$ Hz/photon for the 5626 MHz resonance and $\frac{K'}{2\pi} = -2.4(0.8) \times 10^{-4}$ Hz/photon for the 5689 MHz resonance. For the 5689 MHz resonance we obtain an agreement with the expected theoretical doubling, but for the 5626 MHz resonance there is a discrepancy which might be a result of an additional TLS shift due to non-uniform electric field or imperfections in the calculation of the number of photons at high powers[23]. Similar enhancement of the cross-Kerr shift in comparison to the self-Kerr one was observed with a strong Josephson nonlinearity[33]. Here it is used as a tool for measuring the intrinsic nonlinearity of a presumably linear resonator.

In conclusion, a novel method for the characterization of nonlinearities using a pump-probe scheme on the normal modes of coupled resonators was implemented and analyzed. Using this method the effect of TLS saturation by drive power on the real part of the dielectric constant ϵ was uncovered and the average single photon Rabi frequency of dominant TLSs was extracted. In addition, the Kerr coefficient quantifying the strength of nonlinear kinetic inductance was measured, yielding $\frac{K}{2\pi} \approx -1 \times 10^{-4}$ Hz/photon. Knowledge of the nonlinearities of presumably linear CPWRs down to the single photon limit is important for quantum information applications, such as the implementation of recent proposals for encoding logical qubits by multiphoton cat states[34]. In addition, the

ability to reduce the internal loss of one mode by pumping the other mode can be used to enhance the resonance lifetime while keeping the number of probing photons small, as required e.g. for dispersive readout in circuit QED[26].

[1] M. Göppl, a. Fragner, M. Baur, R. Bianchetti, S. Filipp, J. M. Fink, P. J. Leek, G. Puebla, L. Steffen, and a. Wallraff, Journal of Applied Physics **104**, 113904 (2008), arXiv:0807.4094.

[2] P. K. Day, H. G. LeDuc, B. A. Mazin, A. Vayonakis, and J. Zmuidzinas, Nature **425**, 817 (2003).

[3] M. R. Vissers, J. Hubmayr, M. Sandberg, S. Chaudhuri, C. Bockstiegel, and J. Gao, Applied Physics Letters **107**, 062601 (2015).

[4] P. W. Anderson, B. Halperin, and C. M. Varma, Philosophical Magazine **25**, 1 (1972).

[5] W. Phillips, Journal of Low Temperature Physics **7**, 351 (1972).

[6] W. A. Phillips, Reports on Progress in Physics **50**, 1657 (1987).

[7] J. M. Martinis, K. B. Cooper, R. McDermott, M. Steffen, M. Ansmann, K. D. Osborn, K. Cicak, S. Oh, D. P. Pappas, R. W. Simmonds, and C. C. Yu, Physical Review Letters **95**, 210503 (2005).

[8] M. Von Schickfus and S. Hunklinger, Physics Letters A **64**, 144 (1977).

[9] D. P. Pappas, M. R. Vissers, D. S. Wisbey, J. S. Kline, and J. Gao, IEEE Transactions on Applied Superconductivity **21**, 871 (2011).

[10] M. S. Khalil, F. C. Wellstood, and K. D. Osborn, IEEE Transactions on Applied Superconductivity **21**, 879 (2011).

[11] J. M. Sage, V. Bolkhovsky, W. D. Oliver, B. Turek, and P. B. Welander, Journal of Applied Physics **109**, 063915 (2011), arXiv:1010.6063.

[12] Y. J. Rosen, M. S. Khalil, A. L. Burin, and K. D. Osborn, Physical review letters **116**, 163601 (2016).

[13] S. Skacel, C. Kaiser, S. Wuensch, H. Rotzinger, A. Lukashenko, M. Jerger, G. Weiss, M. Siegel, and A. Ustinov, Applied Physics Letters **106**, 022603 (2015).

[14] Temperature dependence of the resonance frequency in accordance with the standard TLS model was observed e.g. in Refs.[9,11,35]. However, the two-tone pump-probe method deconvolutes the TLS shifts from kinetic inductance effects which might contribute at higher temperatures[36–38]. This is especially relevant for Al which has a low critical temperature. In addition, using the two-tone method one can spatially control the TLS saturation.

[15] Another pair of coupled CPWRs was present on the chip but not used in the experiments.

[16] Notice that the analogy to coupled pendula is not complete. For example, for the pendula the symmetric mode has a lower energy (and frequency) than the anti-symmetric one, while the opposite is true for capacitively coupled resonators.

[17] C. Eichler, Y. Salathe, J. Mlynek, S. Schmidt, and A. Wallraff, Physical Review Letters **113**, 110502 (2014).

[18] E. T. Holland, B. Vlastakis, R. W. Heeres, M. J. Reagor, U. Vool, Z. Leghtas, L. Frunzio, G. Kirchmair, M. H. Devoret, M. Mirrahimi, and R. J. Schoelkopf, Physical review letters **115**, 180501 (2015).

[19] S. Hacohen-Gourgy, V. V. Ramasesh, C. De Grandi, I. Siddiqi, and S. M. Girvin, Phys. Rev. Lett. **115**, 240501 (2015).

[20] M. Khalil, M. Stoutimore, F. Wellstood, and K. Osborn, Journal of Applied Physics **111**, 054510 (2012).

[21] B. A. Mazin, *Microwave kinetic inductance detectors*, Ph.D. thesis, Citeseer (2004).

[22] S. Probst, F. Song, P. Bushev, A. Ustinov, and M. Weides, Review of Scientific Instruments **86**, 024706 (2015).

[23] For more details see supplementary material.

[24] J. Zmuidzinas, Annual Review of Condensed Matter Physics **3**, 169 (2012).

[25] B. Yurke and E. Buks, Journal of Lightwave Technology **24**, 5054 (2006), arXiv:quant-ph/0505018 [quant-ph].

[26] A. Blais, R. S. Huang, A. Wallraff, S. M. Girvin, and R. J. Schoelkopf, Physical Review A - Atomic, Molecular, and Optical Physics **69**, 062320 (2004).

[27] E. T. Jaynes and F. W. Cummings, Proceedings of the IEEE **51**, 89 (1963).

[28] R. Barends, J. Kelly, A. Megrant, D. Sank, E. Jeffrey, Y. Chen, Y. Yin, B. Chiaro, J. Mutus, C. Neill, *et al.*, Physical review letters **111**, 080502 (2013).

[29] J. Wenner, R. Barends, R. C. Bialczak, Y. Chen, J. Kelly, E. Lucero, M. Mariantoni, A. Megrant, P. J. J. O'Malley, D. Sank, A. Vainsencher, H. Wang, T. C. White, Y. Yin, J. Zhao, A. N. Cleland, and J. M. Martinis, Applied Physics Letters **99** (2011), 10.1063/1.3637047, arXiv:1107.4698.

[30] P. De Visser, S. Withington, and D. Goldie, Journal of Applied Physics **108**, 114504 (2010).

[31] A. V. Semenov, I. A. Devyatov, P. J. de Visser, and T. M. Klapwijk, Phys. Rev. Lett. **117**, 047002 (2016).

[32] T. Dahm and D. J. Scalapino, Journal of Applied Physics **81**, 2002 (1997).

[33] E. T. Holland, B. Vlastakis, R. W. Heeres, M. J. Reagor, U. Vool, Z. Leghtas, L. Frunzio, G. Kirchmair, M. H. Devoret, M. Mirrahimi, and R. J. Schoelkopf, Phys. Rev. Lett. **115**, 180501 (2015).

[34] Z. Leghtas, G. Kirchmair, B. Vlastakis, R. J. Schoelkopf,

M. H. Devoret, and M. Mirrahimi, Physical review letters **111**, 120501 (2013).

[35] J. Gao, M. Daal, A. Vayonakis, S. Kumar, J. Zmuidzinas, B. Sadoulet, B. a. Mazin, P. K. Day, and H. G. Leduc, Applied Physics Letters **92**, 152505 (2008).

[36] R. Barends, H. Hortensius, T. Zijlstra, J. Baselmans, S. Yates, J. Gao, and T. Klapwijk, Applied Physics Letters **92**, 223502 (2008).

[37] J. Gao, J. Zmuidzinas, B. Mazin, P. Day, and H. Leduc, Nuclear Instruments and Methods in Physics Research Section A: Accelerators, Spectrometers, Detectors and Associated Equipment **559**, 585 (2006).

[38] H. Wang, M. Hofheinz, J. Wenner, M. Ansmann, R. Bialczak, M. Lenander, E. Lucero, M. Neeley, A. OConnell, D. Sank, *et al.*, Applied Physics Letters **95**, 233508 (2009).